Available online at www.sciencedirect.com

ScienceDirect

Biochimica et Biophysica Acta 1768 (2007) 1138–1146

Biochimica et Biophysica Acta BBA

www.elsevier.com/locate/bbamem

Interaction of piroxicam with mitochondrial membrane and cytochrome *c*

Hirak Chakraborty [a], Prabir K. Chakraborty [b], Sanghamitra Raha [b], Parikshit C. Mandal [a], Munna Sarkar [a,*]

[a] *Chemical Sciences Division, Saha Institute of Nuclear Physics, 1/AF, Bidhannagar, Calcutta-700 064, India*

[b] *Crystallography and Molecular Biology Division, Saha Institute of Nuclear Physics, 1/AF, Bidhannagar, Calcutta-700 064, India*

Received 4 September 2006; received in revised form 5 January 2007; accepted 9 January 2007
Available online 17 January 2007

Abstract

Modulation of surface properties of biomembranes by any ligand leading to permeabilization, fusion, rupture, etc. is a fundamental requirement for many biological processes. In this work, we present the interaction of piroxicam, a long acting Non-Steroidal Anti-Inflammatory Drug (NSAID) with isolated mitochondria, membrane mimetic systems, intact cells and a mitochondrial protein cytochrome *c*. Dye permeabilization study on isolated mitochondria indicates that piroxicam can permeabilize mitochondrial membrane. Direct imaging by Scanning Electron Microscope (SEM) shows that piroxicam induces changes in mitochondrial membrane morphology leading to fusion and rupture. Transmission Electron Microscope (TEM) imaging of piroxicam treated DMPC vesicles and mixed micelles formed from CTAB and SDS show that causing membrane fusion is a general property of piroxicam at physiological pH. In intact cells viz., V79 Chinese Hamster lung fibroblast, piroxicam is capable of releasing cytochrome *c* from mitochondria into the cytosol in a dose dependent manner along with the enhancement of downstream proapoptotic event viz., increase in caspase-3 activity. We have also shown that piroxicam can reduce cytochrome *c* within a time frame relevant to its lifetime in blood plasma. UV-visible spectroscopy has been used to study the reaction mechanism and kinetics in detail, allowing us to propose and validate a Michaelis–Menten like reaction scheme. CD spectroscopy shows that small but significant changes occur in the structure of cytochrome *c* when reduced by piroxicam.

Keywords: NSAIDs; Mitochondria; Membrane fusion; Cytochrome *c*; Kinetics; Optical spectroscopy

1. Introduction

Modification of the surface properties of membranes by any ligand could lead to several phenomena like aggregation, leakage of trapped contents or permeabilization, fusion, etc. Such modulation of surface properties is a fundamental requirement for many biological processes [1]. Piroxicam [4-hydroxy-2-methyl-*N*-(pyridin-2-yl) -2H-1,2-benzothiazine-3-carboxamide 1,1-dioxide], a drug belonging to the oxicam group of NSAIDs, is not only a good anti-inflammatory agent, but also show chemopreventive and chemosuppressive effects in different cancer cell lines and animal models [2–4]. The molecular mechanism behind its anti cancer effect is not yet fully understood. Piroxicam strongly interacts with membrane mimetic systems like micelles and vesicles [5–8]. Different membrane parameters viz. electrostatics and hydrophobicity, affect the transformation or switchover between different prototropic forms of piroxicam in such a way so as to exert a profound effect in dictating which structural form will predominate in solution and would be incorporated in the membrane mimetic systems. To extend our study to biomembranes we chose mitochondrial membrane. Mitochondria are in general a very good pharmacological target [9,10]. It is known that several drugs

Abbreviations: NSAID, Nonsteroidal anti-inflammatory drug; SEM, Scanning electron microscope; TEM, Transmission electron microscope; DMPC, Dimyristoyl phosphatidylcoline; COX, Cyclooxygenase; MOPS, 3-Morpholinopropane sulphonic acid; DMSO, Dimethyl sulfoxide; PBS, Phosphate buffer saline; EGTA, Ethylene glycol-bis(β-aminoethyl ether)-*N,N,N′,N′*-tetraacetic acid; EDTA, Ethylenediaminetetraaceticacid; PTA, Phosphotungstic acid; CD, Circular dichroism; PMSF, Phenylmethylsulfonyl fluoride; PVDF, Polyvinylidene difluoride

* Corresponding author. Fax: +91 33 23374637.
E-mail address: munna.sarkar@saha.ac.in (M. Sarkar).

0005-2736/$ - see front matter © 2007 Elsevier B.V. All rights reserved.
doi:10.1016/j.bbamem.2007.01.004

including NSAIDs can affect the mitochondrial membrane potential, respiration, energy coupling and can also lead to outer membrane permeabilization [9]. Mitochondrial outer membrane permeabilization results in release of proteins like cytochrome *c*, normally found in the space between the inner and outer mitochondrial membranes. Cytochrome *c* release in the cytosol causes caspase activation that orchestrates the downstream events associated with apoptosis [11,12]. Hence, affecting mitochondrial membrane by drugs is an important strategy in chemotherapy [11]. Conventional chemotherapeutic agents result in mitochondrial permeabilization through an indirect way, via pro-apoptotic second messengers, whose nature depends on the apoptosis inducing agent. Such secondary messengers, for example BH3-only members of the Bcl-2 protein family and other proteins, activate the pro-apoptotic BH123 proteins, Bax and Bak, to oligomerize and insert into the outer mitochondrial membrane leading to mitochondrial outer membrane permeabilization [11,12]. This initiates the down-stream cascade of pro-apoptotic events. COX-2 inhibitors like NS-398 and celecoxib have been shown to induce apoptosis mediated by the release of cytochrome *c* from mitochondria with the consequent activation of downstream caspases like caspase-3, caspase-8 and caspase-9, etc. [13,14]. Several different reasons for the release of cytochrome *c* by these COX-2 inhibitors have been proposed, of which modulation of mitochondrial morphology is a possibility.

In this study we are interested to see if piroxicam, a COX-inhibitor, can exert its effect on mitochondrial membrane morphology, thereby leading to the mitochondrial permeabilization. To do so, we have carried out the mitochondrial permeabilization study with cell free isolated mitochondria in presence of piroxicam only. The modulation of mitochondrial membrane morphology by piroxicam has also been directly imaged by Scanning Electron Microscope. To see whether the effect of piroxicam on mitochondrial membrane can have any consequence on cellular processes, we have extended our studies to intact cells. Finally, we show that piroxicam can directly interact with the mitochondrial protein cytochrome *c* in vitro, within a time frame relevant to its lifetime in blood plasma. UV-Visible absorption and CD-spectroscopy have been used to study the slow kinetics of interaction of piroxicam with cytochrome *c*. We are aware that at the cellular level, the effect of piroxicam can also occur via several other parallel pathways e.g., by inducing secondary effectors involved in the physiological control of apoptosis, etc.; but the fusion event observed in the membrane mimetic systems implies that there is a very strong physical interaction of piroxicam with mitochondrial membrane. So, in this study, we only aim to demonstrate the effect of piroxicam at four levels, on isolated mitochondrial membrane, on membrane mimetic systems, on cellular mitochondria and on the mitochondrial protein cytochrome *c*. Identification of pathways other than modulation of mitochondrial morphology for the release of cytochrome *c* and caspase activation in intact cells is the subject of a separate study.

2. Experimental procedures

2.1. Reagents

Piroxicam, DMPC and MOPS were purchased from Sigma Chemicals (US) and were used without further purification. Stock solution of piroxicam of concentration 3 mM was prepared in DMSO (Merck, Germany) and the exact concentration was adjusted by corresponding buffer. Mitotracker Green FM® was purchased from Molecular Probes, USA. Cytochrome *c* and Glycine were purchased from SISCO Research Laboratory (SRL), India.

2.2. Cell culture and treatment

Chinese hamster lung fibroblast V79 cells were grown in minimal essential medium supplemented with 10% fetal bovine serum (Sigma) and antibiotics (penicillin and streptomycin) at 37 °C in a humidified 5% CO_2 atmosphere in plastic petridishes. Cells were grown to confluency and fresh medium was added along with 20, 40 100 μM piroxicam. Equivalent amount of DMSO was added to the control cells to compensate the DMSO present in solution when piroxicam is diluted from stock DMSO solution.

2.3. Immunoblot analysis

After treatment with 1 μM staurosporine (Almone Laboratories, Israel), piroxicam at concentration of 20, 40 and 100 μM respectively, cells were washed in PBS buffer (pH 7.4) and suspended in lysis buffer (20 mM Tris, 1 mM EGTA, 1 mM EDTA, 5 mM NaF and a cocktail of protease inhibitors of 10 μM pepstatin A, 10 μM leupeptin, and 1 mM PMSF, pH 7.5). Cells were ruptured by rapid freeze–thaw and homogenized on ice. Lysed cells and nuclei were pelleted by centrifugation at 1000×*g* for 10 min. The supernatant was centrifuged further at 15000×*g* for 40 min at 4 °C. The resultant supernatant was designated as the cytosolic fraction, which was used for the detection of cytochrome *c*. The supernatant was taken for SDS-polyacrylamide gel electrophoresis (SDS-PAGE). Protein content was quantified according to Bradford [15] and then solubilized in Laemmli sample buffer. The samples were boiled for 5 min at 100 °C and loaded onto a 15% acrylamide gel. Electrophoresis was carried out at a constant voltage of 130 V. Cellular proteins were transferred electrophoretically to a PVDF membrane using an Atto Electroblotter apparatus. The transfer buffer (pH 8.3) contained 96 mM glycine, 10 mM Tris, and 10% methanol. The transfer was carried out for 50 min at constant current of 160 mA. Hydrophobic or nonspecific sites were blocked overnight at 4 °C with 5% BSA in Tris-buffered saline (50 mM Tris and 150 mM NaCl) containing 0.1% Tween 20 (TBS-T). Membranes were washed four times for 15 min in TBS-T. The blots were probed with the primary antibody anti-cytochrome *c* (Cell Signaling Technology, USA) and anti-β-actin (Sigma) in TBS-T, 1% bovine serum albumin for 2 h at room temperature. Membranes were washed four times for 15 min and incubated for 1 h at room temperature with alkaline phosphatase (ALP)-conjugated secondary antibody (1:1000) in TBS-T containing 1% BSA (pH 7.5). Secondary antibodies consisted of ALP-conjugated anti-rabbit IgG (Oncogene Research, USA) for cytochrome *c* and ALP-conjugated anti-mouse IgG for β-actin (Oncogene Research, USA). PVDF membranes were washed four times for 15 min, and cytochrome *c* and β-actin were detected colorimetrically with NBT-BCIP as substrate. Western blots were scanned by a UMAX Astra Scanner and the bands were quantified by using Scion Image Beta 4.02 software from Scion Corporation, USA.

2.4. Isolation of mitochondria

Cells were washed in PBS and suspended in lysis buffer. Cells were ruptured by rapid freeze–thaw and homogenized on ice. Lysed cells and nuclei were pelleted by centrifugation at 1000×*g* for 10 min. The supernatant was centrifuged further at 15,000×*g* for 40 min at 4 °C. Pellet of Mitochondria was collected.

2.5. Measurement of caspase-3 activity

Caspase-3 assay was done by the caspase-3 fluorescence assay kit from BD-Pharmingen, following the protocol mentioned in the kit. Caspase-3 activity is given in arbitrary fluorescence units.

2.6. Fluorescence spectroscopy

Fluorescence measurements were performed using Hitachi spectrofluorimeter model F 4010. All emission spectra were corrected for instrument response at each wavelength. A 2×10 mm^2 path length quartz cell was used for all fluorescence measurements to avoid any blue edge distortion of the spectrum due to inner filter effect [16].

2.7. Scanning electron microscopy

SEM was done using a Quanta 200 FEG model No. D7722 (XTM @ 2001 FEI Company) scanning electron microscope. Samples were spread on the glass cover slip and allowed to dry in room temperature before recording. All samples were recorded at room temperature. We have focused in the region where the salts of buffer were not deposited and clear images of mitochondria were found.

2.8. Transmission electron microscopy

The Transmission Electron Microscopy (TEM) was performed with a Hitachi electron microscope model 600 operating at 75 kV with a resolution of 5 Å. The samples were spread over copper grids coated with carbon. 2% PTA was used as the negative stain for DMPC vesicles.

2.9. UV-Visible absorption spectroscopy

All the absorption spectrum given in different figures were recorded with Thermo Spectronic spectrophotometer model UNICAM UV500. Baseline correction was done with corresponding buffer before recording each set of data. Samples were deoxygenated by passing argon gas for about 20 min before scanning to avoid photochemical changes due to presence of oxygen.

2.10. Circular dichroism

CD spectra were recorded with a Jasco J-720 spectropolarimeter using cylindrical quartz cuvette of path length 2 mm. Each spectrum represents the average of five successive scans performed at a scan speed 20 nm/min. Appropriate baseline subtraction and noise reduction analysis using identical window were performed in each case. All spectra were recorded at 298 K.

3. Results

3.1. Effect of piroxicam on mitochondrial membrane and membrane mimetic systems

In order to study the interaction of piroxicam with mitochondria, experiments were done on mitochondria isolated from cell line V79, Chinese Hamster lung fibroblast, according to the procedure described in Experimental procedures, suspended in PBS buffer (pH 7.4) containing 0.2% (v/v) DMSO. No Ca^{2+} or oxidative substrates were added. Mito Tracker Green FM is a dye used for staining mitochondria. In aqueous buffer, this dye is almost non-fluorescent. On incorporation into mitochondria, it gives a strong fluorescence at an emission maximum of 516 nm [17]. Fig. 1(A) shows the fluorescence spectrum of Mito Tracker Green FM (20 nM) in aqueous buffer and in presence of mitochondria under conditions as mentioned above. To study whether piroxicam is capable of permeabilizing mitochondrial membrane in isolated mitochondria, they were first treated with piroxicam (20 μM) and the fluorescence peak intensity at 516 nm was monitored with time at 37 °C. A decrease in fluorescence intensity would result if the dye were released in aqueous buffer

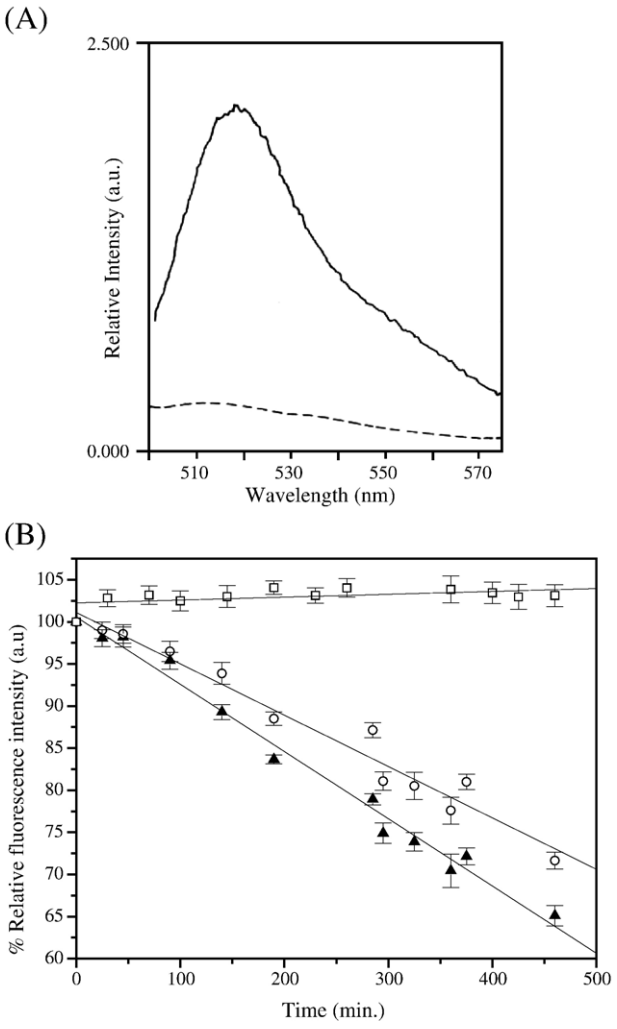

Fig. 1. (A) Fluorescence spectra of MitoTracker Green FM in PBS buffer (- - - - -) and in presence of isolated mitochondria in the same buffer (— —) at pH 7.4, λ_{exc}=490 nm and (B) Plot of % relative fluorescence intensity (at 516 nm) of Mito Tracker Green FM (20 nM) incorporated in mitochondria vs. time in control (○) (correlation coefficient=0.98) and in presence of 20 μM piroxicam (▲) (correlation coefficient=0.99). Plot of % relative fluorescence intensity of Mito Tracker Green FM (20 nM) in presence of piroxicam (20 μM) but in absence of any isolated mitochondria (□). Data are presented as the mean±S.D. for three different experiments.

on mitochondrial membrane permeabilization. Fig. 1(B) shows the time dependent decrease in the intensity of the dye for mitochondria treated with piroxicam and that of the untreated ones. The data presented are the average of three separate experiments. The decrease in the intensity of the dye for piroxicam treated mitochondria is consistently more than that of the control. The difference is around 9% at the end of 7 h. This indicates that the presence of piroxicam results in additional permeabilization with the subsequent release of the dye into the aqueous buffer. In order to see whether this additional decrease in fluorescence intensity of the dye, in presence of piroxicam, is not due to direct quenching of the dye by piroxicam, the interaction of piroxicam with the dye in absence of isolated mitochondrion was followed for the same time period. The experimental conditions and concentrations of the dye and

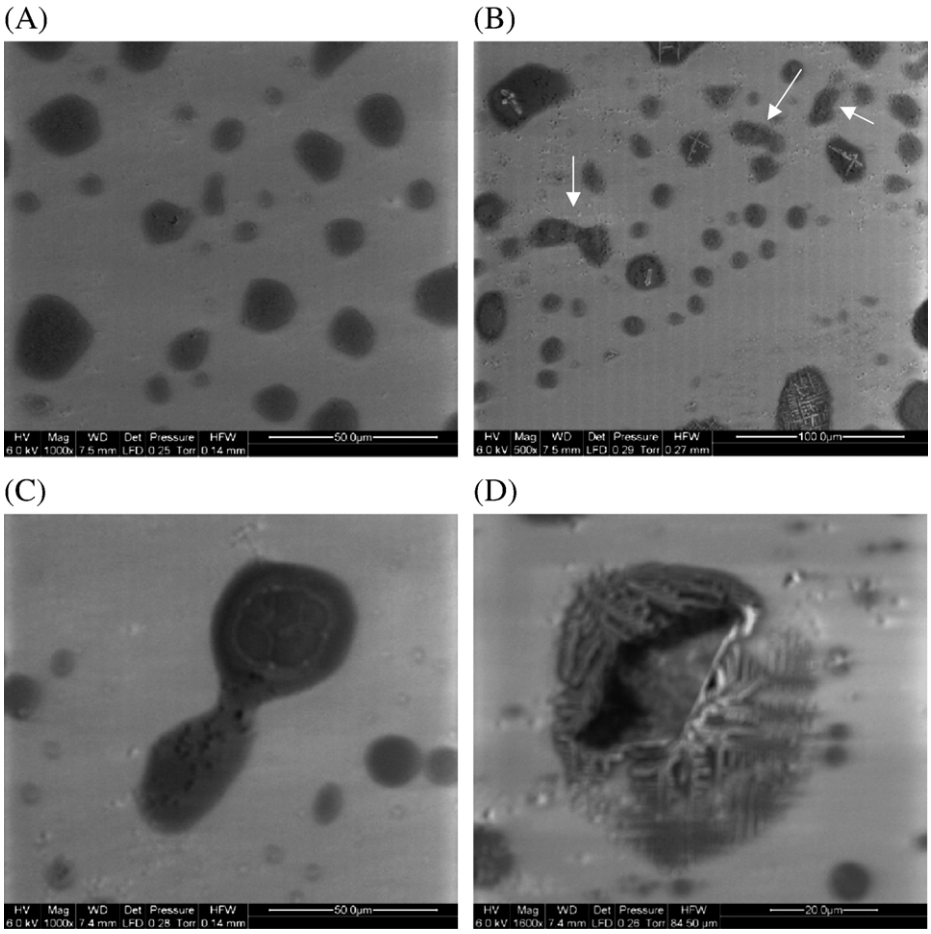

Fig. 2. SEM photograph of (A) isolated mitochondria in PBS buffer at pH 7.4 without adding piroxicam (B) after 5 h incubation with 20 μM piroxicam, (C) enlarged image of a fused mitochondria, (D) enlarged image of a typical ruptured mitochondria.

piroxicam were kept identical as in case of the experiment with isolated mitochondria. It is evident from Fig. 1(B) that no interaction between piroxicam and MitoTracker Green FM occurs within the time frame studied, resulting in no significant change in the fluorescence intensity of the dye. This clearly shows that the decrease in the fluorescence intensity of the dye in presence of the drug is due to release of the dye from the mitochondria into the aqueous buffer. The 9% additional decrease in the intensity for piroxicam treated mitochondria compared to that of the control is small but significant.

Scanning electron microscope was used to image directly the effect of piroxicam on isolated mitochondria,. Fig. 2(A–D) show SEM photographs of isolated mitochondria for both untreated and treated with piroxicam. Fig. 2(A) is that of the isolated mitochondria in absence of piroxicam, whereas Fig. 2 (B) shows the SEM photograph of the same mitochondria as Fig. 2(A) but treated with 20 μM piroxicam for 5 h. Fig. 2(B) clearly shows the presence of fused mitochondria indicated by white arrows. This is not seen in Fig. 2(A). A fused mitochondria is enlarged in Fig. 2(C). The typical dumbbell shape characterized by the presence of a 'stalk' between two fused mitochondria is similar to that proposed/ observed in Case of fusion of other membrane mimetic systems [18,19]. Fig. 2(D) is the enlarged SEM photograph of a ruptured mitochondria. It should be mentioned, that for untreated mitochondria as shown in Fig. 2(A), there exist no fused bodies or ruptured mitochondria. However due to the stringent condition imposed on the system to record the SEM photographs (mentioned in Experimental procedures), there has been significant swelling in the volume of mitochondria. This is obvious in the heterogeneity of the sizes as seen in Fig. 2(A). In order to demonstrate that the change brought about in the morphology of mitochondrial membrane is a general property of piroxicam, studies were carried out on membrane mimetic systems, viz., mixed micelles and liposomes. Fig. 3(a) shows the transmission electron micrograph of mixed micelles formed from 0.1 mM CTAB and 15 mM SDS, in absence [Fig. 3a(i)] and in presence of 30 μM piroxicam [Fig. 3a(ii)], incubated for 2 h. The TEM photograph of mixed micelles in absence of piroxicam is clearly a poly disperse solution without any fusion bodies. When the same mixed micellar system was treated with 30 μM piroxicam, several fusion bodies appeared. The typical 'ball and stalk' figure characteristics of hemi-fusion is seen indicating that the drug can induce fusion in mixed micellar system. Similar observation was made in case of DMPC liposomes. Fig. 3b(i) shows the TEM photograph of untreated DMPC liposomes. No

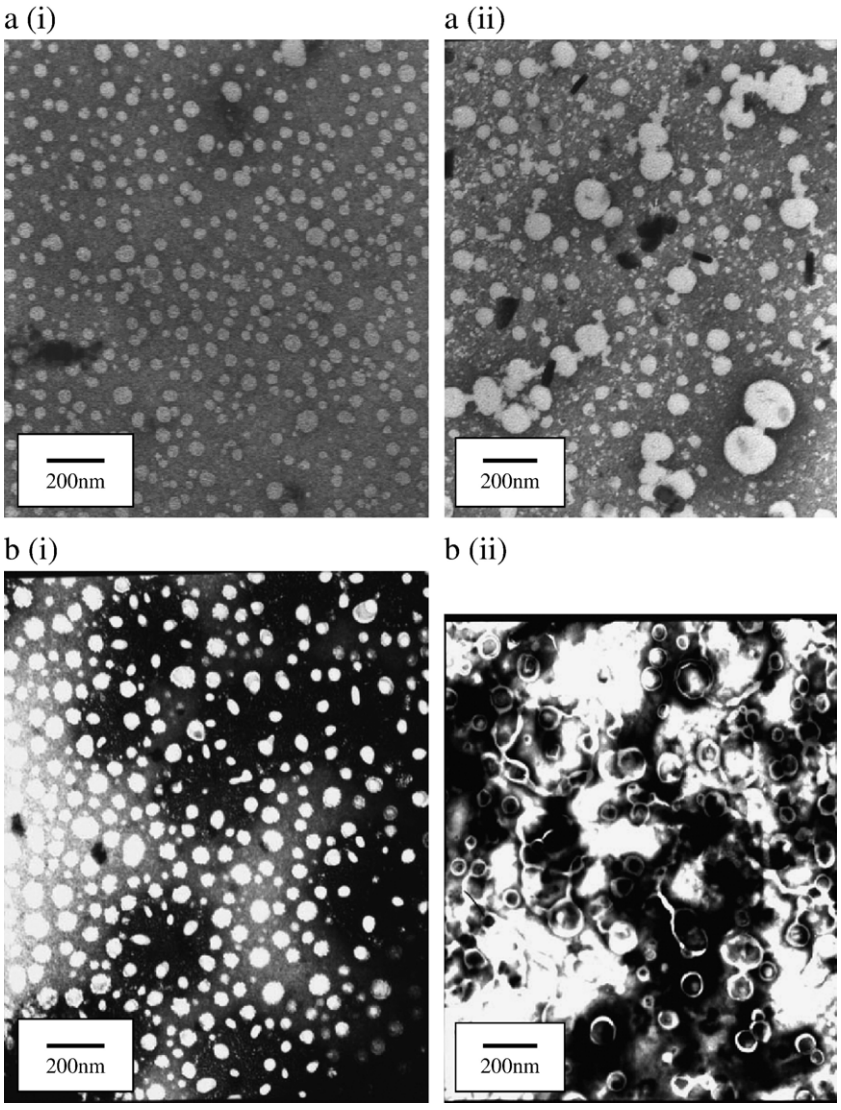

Fig. 3. TEM photograph of [a(i)] mixed micelles of 0.1 mM CTAB and 15 mM SDS at pH 7.4, [a(ii)] mixed micelles of same composition incubated with 30 μM piroxicam for 2 h, [b(i)] DMPC vesicles in MOPS buffer at pH 7.4 [b(ii)] DMPC vesicles incubated for 2 h with 30 μM piroxicam at pH 7.4.

fusion body is seen in the micrograph. Fusion occurs on treating the DMPC liposomes with 30 μM piroxicam as is evident in Fig. 3b(ii). Figs. 2 and 3 indicate that induction of membrane fusion is a general property of piroxicam. It is this fusogenic property that allows the drug to change the mitochondrial membrane morphology leading to fusion and subsequent rupture.

3.2. Piroxicam induced cytochrome c release and Caspase-3 activation in V79 Chinese hamster lung fibroblast cell

The results presented above lead to the question whether modulation of mitochondrial membrane by piroxicam can have any consequence at the cellular level. Studies were carried out on V79 Chinese Hamster Lung Fibroblast cell line, the same cell line used to isolate mitochondria for the experiments mentioned in the previous section. Cells were incubated in absence and in presence of piroxicam at increasing doses of 20, 40 and 100 μM for a period of 8 h. A positive control for cytochrome *c* release is included using 1 μM staurosporine treated cells under identical condition. The treated and untreated cells were ruptured and immunoblot analysis for the detection of cytochrome *c* was performed on the cytosolic fraction. It is clear that in piroxicam treated cells, cytochrome *c* is released in the cytosol in a dose dependent manner (Fig. 4A). Fig. 4C shows the band intensity of the released cytochrome *c*. Cytochrome c release from mitochondria is known to activate caspases that orchestrate the downstream events associated with apoptosis. Fig. 4(D) shows the corresponding increase in caspase-3 activity of V79 cells treated with increasing concentration of piroxicam. The increase in caspase-3 activity also occurred in a dose dependent manner. Release of cytochrome *c* in the cytosol by piroxicam can occur by different pathways, but our results indicate that direct modulation of mitochondrial morphology by the drug could also be one of the possibilities.

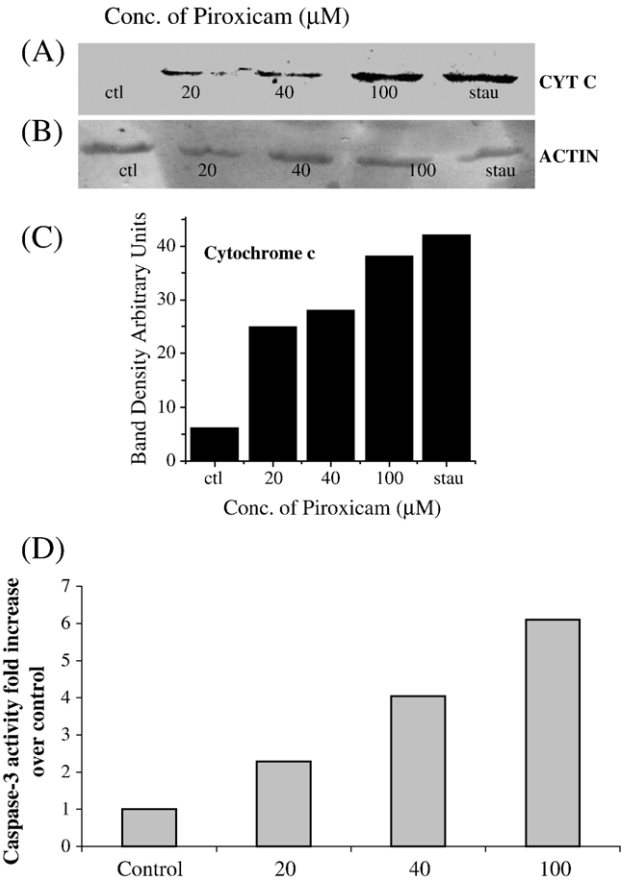

Fig. 4. Cytochrome *c* release and caspase-3 activation by piroxicam in V79 fibroblasts. (A) Untreated (control) and treated with 20, 40 and 100 μM piroxicam or 1 μM staurosporine probed with anti-cytochrome *c*. The experiments were repeated three times. (B) An immunoblot of cytosolic fractions isolated form V79 fibroblasts either untreated (control) or treated with 20, 40 and 100 μM piroxicam or 1 μM staurosporine probed with anti-β-actin antibodies. (C) Band density of cytochrome *c* either untreated (control) or treated with 20, 40 and 100 μM piroxicam or 1 μM staurosporine, (D) Caspase-3 activity in V79 fibroblasts either untreated (control) or treated with 20, 40 and 100 μM piroxicam. Caspase-3 activity is given number of folds increase in caspase-3 activity over control. Data are presented as the mean for three different experiments.

3.3. Interaction of piroxicam with cytochrome c

After demonstrating the effect of piroxicam on the morphology of mitochondrial membrane and membrane mimetic systems as well as its effect on intact cells, we extend our work to see if the drug can interact with cytochrome *c*. In the previous section we have shown that piroxicam is capable of releasing cytochrome *c* from the mitochondria. One of the mechanisms as proposed by us is the direct modulation of the mitochondrial membrane leading to permeabilization. In this section we show that piroxicam can directly interact with cytochrome *c* leading to the reduction of its heme group. The kinetics and the mechanism of this interaction are also presented in this section.

Fig. 5(A) shows the absorption spectrum in the region 500 nm to 600 nm of the mixture of cytochrome *c* (5 μM) and piroxicam (50 μM), recorded immediately after mixing and after a time period of 6 h. The concentration of 50 μM is within the dose range in which piroxicam can affect the mitochondria in intact cells as shown in Fig. 4. It should be mentioned that the same effect of piroxicam on cytochrome *c* was seen at lower concentration of 20 μM. Data are presented for the higher dose of 50 μM which has a better signal to noise ratio. For all experiments the pH of the solution is maintained at 7.4. Two peaks at 520 nm and 550 nm replace the broad band between 500–600 nm in the spectrum recorded after 6 h. These two peaks are characteristics of reduced heme group [Fe(II)] of cytochrome *c* [20], which indicates that piroxicam is capable of slowly reducing cytochrome *c*. The absorption maximum of the anionic form (predominant form of piroxicam at pH 7.4) of piroxicam is at 356 nm. This peak is strongly reduced in the spectrum recorded after 6 h (data not shown). It should be mentioned that the disappearance of the 356 nm band and the appearance of 520 nm and 550 nm doublet do not occur

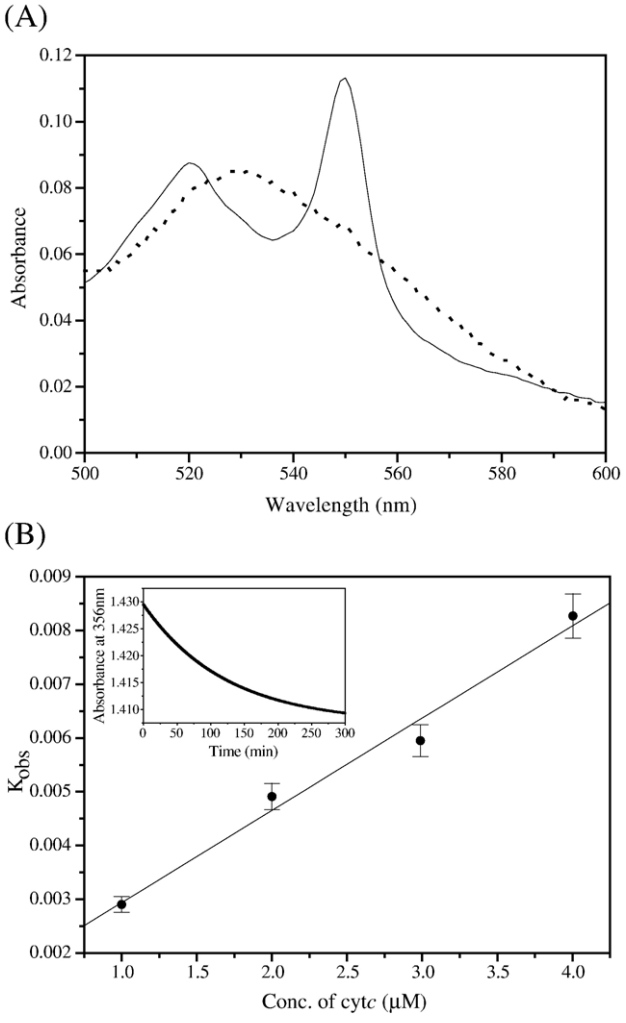

Fig. 5. (A) Absorption spectra of a mixture of 50 μM piroxicam and 5 μM cytochrome *c* in MOPS buffer (pH 7.4) just after the mixing (……..) and after 6 h of mixing (——), (b Inset) Plot of absorbance at 356 nm vs. time, a representative decay profile when concentration of piroxicam was 50 μM and cytochrome *c* was 5 μM and (B) Plot of K_{obs} vs. concentration of cytochrome *c* at pH 7.4 and 37 °C (correlation coefficient = 0.99). Data are presented as the mean ± S.D. for three different experiments.

simultaneously. Decrease in the absorbance at 356 nm was therefore monitored to study the reaction kinetics of the first phase of the above reaction. Fig. 5(B) inset shows a plot of absorbance at 356 nm vs. time. It is evident that the decay profile follows first order reaction kinetics and hence the rate constant of the reaction (K_{obs}) can be calculated from the fitting of the absorbance at 356 nm vs. time (min.) plot to the following equation

$$O.D_t = A_0 + A_1 \times \exp(-K_{obs} \times t),$$

where 'O.D$_t$' is the absorbance at 356 nm at time t, A_0 and A_1 are constants, K_{obs} is the rate constant of the reaction and t is the time in min. The K_{obs} was followed with increasing concentration of cytochrome *c,* keeping the concentration of piroxicam at least 10-fold more. The linear dependence of K_{obs} on the concentration of cytochrome *c,* as shown in Fig. 5(B), has a non-zero intercept. This indicates that the reaction between piroxicam and cytochrome *c* is reversible. As has been mentioned before, the disappearance of the peak at 356 nm for anionic piroxicam is not followed by concomitant increase of the peak at 550 nm belonging to that of reduced cytochrome *c*. This is suggestive of the fact that the reaction between piroxicam and cytochrome *c* proceeds through the formation of an intermediate. Since no new band of the intermediate develops at any point of time it is obvious that the absorption of the intermediate overlaps with the reactants and / or products. Hence it was not possible to directly follow the formation as well as the disappearance of the intermediate spectrophotometrically. The late onset of the 550 nm band of reduced cytochrome *c* shows that the disappearance of the intermediate might be the slowest step and hence the rate determining step of the whole reaction. The rate of reduction of cytochrome *c* was measured by monitoring the increase of absorbance at 550 nm. Keeping in mind the results of Fig. 5(B) inset and Fig. 5(B) and the above facts, we propose the following scheme of reaction.

$$(CytC)_{ox} + Px \underset{k_{-1}}{\overset{k_1}{\rightleftarrows}} [(CytC)_{ox} - Px] \xrightarrow{k_2} Product + (CytC)_{red}$$

The above scheme is a Michaelis–Menten like reaction. Under the condition of [Px]>>[Cytc] (at least 10-fold) the rate of formation of reduced cytochrome *c* is dependent on the concentration of piroxicam at a particular concentration of cytochrome *c*. The rate (v) can then be expressed by the following reaction,

$$\frac{1}{v} = \frac{1}{V_{max}} + \frac{K_M}{V_{max}[Px]} \quad (1)$$

where v is the rate of the reaction, V_{max} is the maximum velocity for the steady state conversion of the substrate into product and K_M is the Michaelis constant for the substrate. So the plot of $1/v$ vs. $1/[Px]$ will give a straight line, which allows us to determine the values of K_M and V_{max}.

Fig. 6(A) shows the plot of $1/v$ vs. $1/[Px]$. v was measured at 550 nm, which is the characteristic absorption maximum of reduced cytochrome *c*. For each point, data were recorded thrice and the error bar gives the standard deviation. The value of K_M and V_{max} were calculated from Fig. 6(A) and were found to be 121.6 μM and 4.21×10^{-4} μM min^{-1} respectively. The K_M value is of intermediate range, which indicates that the dissociation of the intermediate (Px–CytC complex) is thermodynamically favorable but the low value of V_{max} indicates slow rate of dissociation.

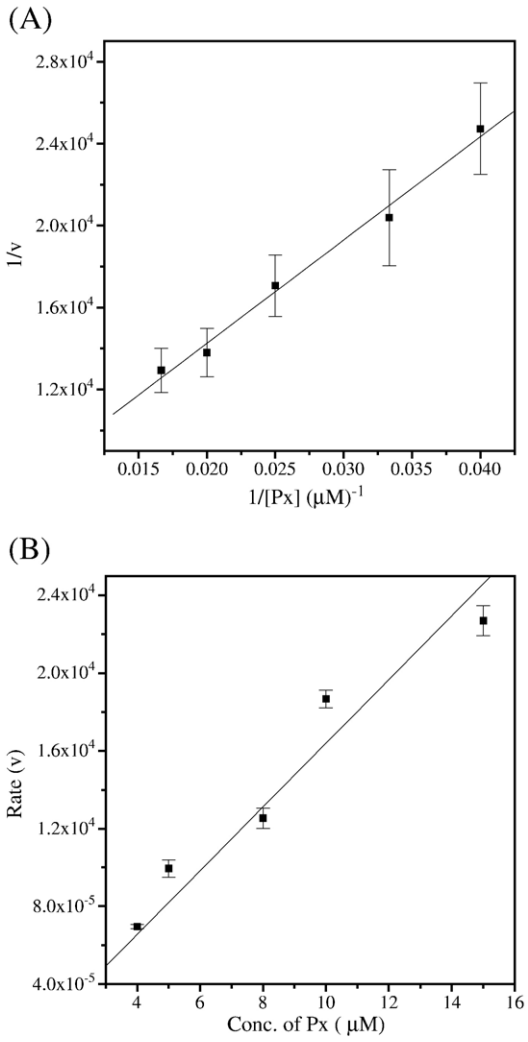

Fig. 6. (A) Plot of $1/v$ vs. $1/[Px]$ for [Px]>>[Cytc] (correlation coefficient=0.99) and (B) Plot of v vs. [Px] for [Px]<<[Cytc] (correlation coefficient=0.97), velocity of the reaction (v) was measured at 550 nm, which is the characteristic absorption maximum of reduced cytochrome *c*. Data are presented as the mean±S.D. for triplicate experiments.

As a double check we have also followed the kinetics under the condition [Px]<<[CytC] (10-fold). The rate of formation of reduced cytochrome *c* is then dependent on the concentration of piroxicam at a particular concentration of cytochrome *c* in the following manner,

$$v = \frac{k_2[CytC][Px]}{K_M} \quad (2)$$

Fig. 6(B) shows the plot of v vs. [Px], which is linear as expected from the above equation and the rate of the reaction is

first order with respect to the piroxicam concentration. Fig. 6(A) and 6(B) show that our assumption of a reaction scheme, which is Michaelis–Menten like, is the true representation of the reaction mechanism between piroxicam and cytochrome *c*.

There exists a controversy as to whether the structure of cytochrome *c* is also altered when the heme group is reduced [21,22]. Several studies have been devoted to this. In order to see whether reaction with piroxicam can alter the structure of cytochrome *c* along with the reduction of heme group, CD spectrum of piroxicam and cytochrome *c* mixture was recorded immediately after mixing, after 3 h of mixing and after 6 h. Reduction of 222 nm and 208 nm peak characteristic of α-helix shows that the reaction with piroxicam results in small but significant changes in the protein conformation along with the reduction of Fe(III) (Fig. 7).

4. Discussion

Our results demonstrate the effect of piroxicam on mitochondrial membrane morphology, on membrane mimetic systems, on intact cells and on cytochrome *c*, a mitochondrial protein. Piroxicam is a long acting NSAID taking about 6 h to achieve peak plasma concentration and 40–50 h for complete metabolism [23]. The normal plasma level of piroxicam is 8 μg/ml, which is 24 μM. The effects exhibited by the drug as described in results occur at physiologically relevant concentration and time frame.

The results on isolated mitochondria indicate that mitochondria can be permeabilized by piroxicam. The SEM images show that piroxicam can directly affect mitochondrial membrane leading to fusion and rupture. Studies on membrane mimetic systems like DMPC liposomes and mixed micelles show that, causing membrane fusion is a general property of piroxicam. Several models have been proposed to explain membrane fusion and fusion of membrane mimetic systems by different fusogenic agents like PEG [24], viral fusion peptide [25], SNARE proteins [26], etc. Membrane perturbation by fusogenic agent is a pre-requisite for membrane fusion. The extent of perturbation directly correlates with the fusogenic ability of the inducing agent [27–29]. A membrane fusion is a three-step process: aggregation, followed by disrupted packing in the contacting bilayer to form the 'stalk' and finally mixing of vesicles contents. It is interesting to speculate on the mechanism by which piroxicam can induce fusion in membrane mimetic systems and mitochondrial membranes. It is reported that piroxicam can decrease the transition temperature of DPPC bilayers [30]. A decrease in transition temperature of phospholipid reflects a disordering effect of the drug on the lipid bilayer [30]. This disordering could lead to decrease in rigidity of the drug populated vesicles such that it is highly plausible that random collisions of two such vesicles becomes less elastic, thereby increasing the propensity for aggregation followed by fusion. Membrane fusion property of a NSAID has not been demonstrated before and to our knowledge, this is the first report on the fusogenic property of a NSAID.

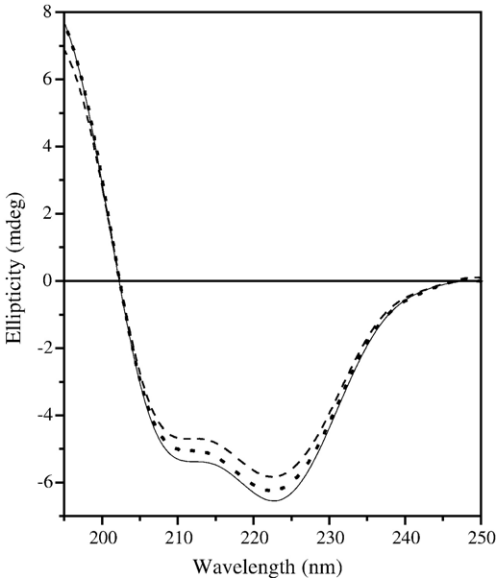

Fig. 7. Circular Dichroism spectra of piroxicam (50 μM)-cytochrome *c* (5 μM) mixture just after mixing (———), after 3 h of incubation (… … .) and after of 6 h of incubation (- - - - - - -).

Modulation of mitochondrial membrane morphology by piroxicam leading to permeabilization seems to have consequences at the cellular level as seen from our studies on V79 Chinese Hamster fibroblasts. It is clearly seen that piroxicam can permeabilize mitochondrial membrane and release cytochrome *c* in a dose dependent manner. Release of cytochrome *c* in the cytosol is known to activate caspases that orchestrates the downstream events that lead to apoptosis. Here we show the increase in caspase-3 activity by piroxicam, which indicates the initiation of pro-apoptotic downstream events. Mitochondrial membrane permeabilization leading to cytochrome *c* release has been proposed to occur by different pathways viz., (a) by swelling of the outer membrane [31–33]; (b) mitochondrial transition pore (PTP) opening along with the association of pro-apoptotic protein like Bax [34,35]; (c) alteration of mitochondrial membrane morphology. It should be mentioned that cytochrome *c* release from mitochondria, achieved by secondary effectors like proapoptotic Bax protein has not been probed in this work. We only point out that modulation of mitochondrial morphology could be one of the many different ways that piroxicam can permeabilize mitochondria in intact cells. Interaction of piroxicam with cytochrome *c* indicates that the drug can slowly reduce the heme group [Fe(III) to Fe(II)] within a time frame relevant to its lifetime in blood plasma. This is not surprising considering that piroxicam can act as an effective antioxidant agent [36,37], which reflects its capacity as a reducing agent. We have proposed a scheme of reaction mechanism, which involves an intermediate that could not be spectroscopically determined. Despite that, our results on the kinetics validate the existence of such intermediate. The Michaelis–Menten like reaction scheme as proposed here adequately fits to our kinetics data. It should be pointed out that small structural changes as followed by CD-measurements is seen in the cytochrome *c* with the alteration of its redox state by piroxicam. This is consistent with the recently reported study

by Sagle et al. [38] which shows that parts of cytochrome *c* exist in dynamic equilibrium with locally unfolded state, which in turn is dependent on the protein's oxidation state.

Finally, we have been able to demonstrate that membrane fusogenic property of piroxicam leads to permeabilization of mitochondrial membrane. We propose that one of the possible pathways by which piroxicam permeabilizes mitochondria leading to release of cytochrome *c* and subsequent caspase-3 activation is by modulation of mitochondrial membrane morphology. We also demonstrate that piroxicam can reduce cytochrome *c* by a slow kinetics, which follows a Michaelis–Menten like reaction scheme leading to small structural changes to the protein itself.

References

[1] R. Jahn, T. Lang, T.C. Sudhof, Membrane fusion, Cell 112 (2003) 519–533.
[2] M.B. Sporn, N. Suh, Chemoprevention of cancer, Carcinogenesis 21 (2000) 525–530.
[3] S.R. Ritland, S.J. Gendler, Chemoprevention of intestinal adenomas in the APC^{min} mouse by piroxicam: kinetics, strain effects and resistance to chemoprevention, Carcinogenesis 20 (1999) 51–58.
[4] E.M. Grossman, W.E. Longo, N. Panesar, J.E. Mazuski, D.L. Kaminshi, The role of cyclooxygenase enzyme in the growth of human gall bladder cancer cells, Carcinogenesis 21 (2000) 1403–1409.
[5] H. Chakraborty, M. Sarkar, Optical spectroscopic and TEM studies of catanionic micelles of CTAB/SDS and their interaction with a NSAID, Langmuir 20 (2004) 3551–3558.
[6] H. Chakraborty, R. Banerjee, M. Sarkar, Incorporation of NSAIDs in micelles: implication of structural switch over in drug–membrane interaction, Biophys. Chem. 104 (2003) 315–325.
[7] H. Chakraborty, S. Roy, M. Sarkar, Interaction of oxicam NSAIDs with DMPC vesicles: differential partitioning of drugs, Chem. Phys. Lipids 138 (2005) 20–28.
[8] H. Chakraborty, M. Sarkar, Interaction of piroxicam with micelles: effect of hydrophobic chain length on structural switchover, Biophys. Chem. 117 (2005) 79–85.
[9] A. Szewczyk, L. Wojtczak, Mitochondria as a pharmacological target, Pharmacol. Rev. 54 (2002) 101–127.
[10] P. Costantini, E. Jacotot, D. Decaudin, G. Kroemer, Mitochondrion as a novel target of anticancer chemotherapy, J. Natl. Cancer Inst. 92 (2000) 1042–1052.
[11] X. Jiang, X. Wang, Cytochrome c-mediated apoptosis, Annu. Rev. Biochem. 73 (2004) 87–106.
[12] D.R. Green, G. Kroemer, The pathophysiology of mitochondrial cell death, Science 305 (2004) 626–629.
[13] M. Li, X. Wu, X. Xu, Induction of apoptosis in colon cancer cells by cyclooxygenase-2 inhibitor NS398 through a cytochrome *c* dependent pathway, Clin. Can. Res. 7 (2001) 1010–1016.
[14] V. Jendrossek, R. Handrick, C. Belka, Celecoxib activates a novel mitochondrial apoptosis signaling pathway, FASEB J. 17 (2003) 1547–1550.
[15] M.M. Bradford, A rapid and sensitive method for the quantification of microgram quantities of protein utilizing the principle of protein-dye binding, Anal. Biochem. 72 (1976) 248–254.
[16] J.R. Lakowicz, Principles of fluorescence spectroscopy, Kluwer Academic/Plennum Publishers, New York, 1999.
[17] J.F. Keij, C. Bell-Prince, J.A. Steinkamp, Staining of mitochondrial membranes with 10-nonyl acridine orange MitoFluor Green and MitoTracker Grees is affected by mitochondrial membrane potential altering drugs, Cytometry 39 (2000) 203–210.
[18] B.R. Lentz, V. Malinin, M.E. Haque, K. Evans, Protein machines and lipid assemblies: current views of cell membrane fusion, Curr. Opin. Struc. Biol. 10 (2000) 607–615.
[19] D.P. Pantazatos, R.C. McDonald, Directly observed membrane fusion between oppositely charged phospholipid bilayers, J. Mem. Biol. 170 (1999) 27–38.
[20] M. Braun, L. Thony-Meyer, Biosynthesis of artificial microperoxidases by exploiting the secretion and cytochrome *c* maturation apparatuses of *Escherichia coli*, Proc. Natl. Acad. Sci. U. S. A. 101 (2004) 12830–12835.
[21] J.F. Clvert, J.L. Hill, A. Dong, Redox-dependent conformational changes are common structural features of cytochrome *c* from various species, Arch. Biochem. Biophys. 346 (1997) 287–293.
[22] T. Takano, R.E. Dickerson, Conformation change of cytochrome *c*: I. Ferrocytochrome *c* structure refined at 1.5 Å resolution, J. Mol. Biol. 153 (1981) 79–94.
[23] http://www.rxlist.com/cgi/generic/piroxicam_cp.htm.
[24] K.O. Evans, B.R. Lentz, Kinetics of lipid rearrangement during poly (ethylene glycol)-mediated fusion of highly curved unilamellar vesicles, Biochemistry 41 (2002) 1241–1249.
[25] S.M. Dennison, N. Greenfield, J. Lenard, B.R. Lentz, VSV transmembrane domain (TMD) peptide promotes PEG-mediated fusion of liposome in a conformationally sensitive fashion, Biochemistry 41 (2002) 14925–14934.
[26] Y. Wang, G.A. Grabowski, X. Qi, Phospholipid vesicle fusion induced by saposin C, Arch. Biochem. Biophys. 415 (2003) 43–53.
[27] P. Bonnafous, T. Stegmann, Membrane perturbation and fusion pore formation in influenza hemagglutinin-mediated membrane fusion, J. Biol. Chem. 275 (2000) 6160–6166.
[28] J. Zhao, S. Kimura, Y. Imanishi, Fusion of liposomes due to transient and lasting perturbation induced by synthetic amphiphilic peptides, Biochim. Biophys. Acta 1283 (1996) 37–44.
[29] J.L. Swift, A. Carnini, T.E.S. Dahms, D.T. Cramb, Anesthetic-enhanced membrane fusion examined using two-photon fluorescence correlation spectroscopy, J. Phys. Chem., B 108 (2004) 11133–11138.
[30] I. Kyrikou, S.K. Hadjikakou, D. Kovala-Demertzi, K. Viras, T. Mavromoustakos, Effects of non-steroid anti-inflammatory drugs in membrane bilayers, Chem. Phys. Lipids 132 (2004) 157–169.
[31] J.L. Scarlet, M.P. Murphy, Release of apoptogenic proteins from the mitochondrial intermembrane space during the mitochondrial permeability transition, FEBS Lett. 418 (1997) 282–286.
[32] M.G. Vander Heiden, N.S. Chandel, E.K. Williamson, P.T. Schumacker, C.B. Thompson, Bcl-X_L regulates the membrane potential and volume homeostasis of mitochondria, Cell 91 (1997) 627–637.
[33] P.X. Petit, M. Gouben, P.P. Diolez, S.A. Susin, G. Kroemer, Disruption of the outer mitochondrial membrane as result of large amplitude swelling: the impact of irreversible permeability transition, FEBS Lett. 426 (1998) 111–116.
[34] I. Marzo, C. Brenner, G. Kroemer, The central role of mitochondria megachannel in apoptosis: evidence obtained with intact cells, mitochondria and purified protein complexes, Biomed. Pharmacother. 51 (1998) 248–251.
[35] M. Crompton, The mitochondrial permeability transition pore and its role in the cell death, Biochem. J. 341 (1999) 233–249.
[36] P.V. Antwerpen, J. Neve, In vitro comparative assessment of the scavenging activity against three reactive oxygen species of non-steroidal anti-inflammatory drugs from the oxicam and sulfoanilide families, Euro. J. Pharm. 496 (2004) 55–61.
[37] Y. Oyanagui, M. Taniguchi, M. Iwata, M. Murakami, Inhibition of immunoglobulin G-catalyzed hydrogen peroxide generation by dexamethasone and piroxicam, Life Sci. 73 (2003) 1333–1346.
[38] L.B. Sagle, J. Zimmermann, S. Matsuda, P.E. Dawson, F.R. Romesberg, Redox-coupled dynamics and folding in cytochrome *c*, J. Am. Chem. Soc. 128 (2006) 7909–7915.